Toward A More Comprehensive Approach for Design Using Buckling Analysis

Oğuzhan Toğay[1], Woo Yong Jeong[2], Cliff D. Bishop[3], Donald W. White[4]

Abstract
This paper discusses a comprehensive approach for the design checking of structural steel members and their bracing systems via the use of buckling analysis combined with appropriate column or beam stiffness reduction factors. The stiffness reduction factors are derived from the AISC column and lateral torsional buckling strength curves. The resulting analysis provides a direct check of the member design resistance without the need for separate checking of the underlying Specification limit state equations. In addition, it can be used to directly evaluate stability bracing stiffness requirements. The paper presents the stiffness reduction factor equations for both columns and beams, and explains how these factors can be incorporated into a buckling analysis calculation. The paper closes with a representative beam design example.

1. Introduction

Within the context of the Effective Length Method of design (the ELM), engineers have often calculated inelastic buckling effective length (K) factors to achieve a more accurate and economical design of columns. This process involves the determination of a stiffness reduction factor, τ, which captures the loss of rigidity of the column due to the spread of plasticity, including initial residual stress effects, as a function of the magnitude of the column axial force. Several different tau factor equations are in use in practice, but there is only one that fully captures the implicit inelastic stiffness reduction associated with the AISC column curve. This tau factor typically is referred to as τ_a. What many engineers do not realize is that the ELM does not actually require the calculation of K factors at all. The column theoretical buckling load can be calculated directly and used in the design equations rather than being determined implicitly via the use of K. Furthermore, if the stiffness reduction 0.9 x 0.877 x τ_q is incorporated within a direct buckling analysis, the calculations may be set up such that, if the member or structure buckles a given multiple of the required design load, γP_u in LRFD, the load γP_u is equal to $\phi_c P_n$. If the load multiplier γ corresponding to the buckling load is greater than 1.0, with the column stiffnesses calculated based on 0.9 x 0.877 x τ_a, the member or structure satisfies the AISC Specification column strength requirements without the need for further checking. The column strength requirements are inherently included the buckling calculations.

---

[1] Graduate Research Assistant, Georgia Institute of Technology, <oguzhantogay@gatech.edu>
[2] Graduate Research Associate, Georgia Institute of Technology, <wyjeong77@gmail.com >
[3] Associate, Exponent, Inc., <cbishop@exponent.com>
[4] Professor, Georgia Institute of Technology, <don.white@gatech.edu>

The above approach can be applied not only to account for column end rotational restraint from supports or other structural framing. In addition, it can be employed to directly evaluate the column strength given the modeled stiffness of any type or combination of bracing. Furthermore, since the bracing stiffness requirements of the AISC Specification Appendix 6 are based on multiplying the *ideal* bracing stiffness, which is the bracing stiffness necessary to achieve a column buckling strength equal to the required column axial load, by $2/\phi = 2/0.75$ in LRFD, a buckling analysis that incorporates the column τ_a factor(s) can be used as a direct method to design column stability bracing. Even more exiting and powerful is that the above approach can be extended to the member and stability bracing design of beams and beam-columns.

This paper reviews the development and proper use of the column stiffness reduction factor, τ_a. However, the major focus of the paper is the extension of the column buckling analysis procedures based on τ_a to the assessment of I-section beam lateral torsional buckling as well as I-section beam stability bracing. A representative beam design and stability bracing example is presented, and the results of this design are compared to the results from rigorous test simulations.

2. Methodology
2.1 Column Inelastic Buckling Analysis using the AISC Inelastic Stiffness Reduction Factor τ_a
The column inelastic stiffness reduction factor τ_a is the most appropriate of various options for column stiffness reduction estimates for design assessment of steel columns via a buckling analysis. This is because τ_a is derived directly from the AISC column strength curve. Therefore, when configured properly with a buckling analysis, the internal axial force in the column(s) is equal to $\phi_c P_n$ at incipient buckling of the analysis model. The τ_a factor accounts implicitly for residual stress effects and initial geometric imperfection effects, as well as the traditional higher margin of safety specified by AISC for slender columns. This factor is *not* the most appropriate inelastic stiffness reduction for a second-order load-deflection analysis, such as an analysis conducted to satisfy the requirements of the Direct Analysis Method of design (the DM). The τ_b factor has been adopted by AISC for use with the Direct Analysis Method. The τ_b factor essentially only accounts for nominal residual stress effects. If used with a second-order analysis per the DM, the τ_a factor gives falsely low strength predictions. This is because the engineer would effectively be double-counting geometric imperfection effects in the DM if τ_a were used, since geometric imperfections are explicitly modeled as part of the DM. (τ_a could still be used as part of a separate out-of-plane stability check in planar analysis and design cases where the DM is used for assessing the internal forces and the in-plan limit states.) The use of τ_a in an buckling analysis allows the engineer to obtain a reasonable prediction of column strengths without needing to run a more elaborate second-order load-deflection analysis.

The τ_a factor has been used extensively for the calculation of column inelastic effective length factors for use in the AISC Effective Length Method of design (the ELM). However, as has been well documented throughout the literature, one does not have to actually calculate column effective lengths to use the ELM. The ELM can be employed with an explicit buckling analysis to determine the column internal axial force at theoretical buckling, P_e, or the corresponding column axial stress F_e (in essence a "direct" buckling analysis, but the word "direct" is being

avoided here to avoid confusion with the DM). This type of application of the ELM, including the application of τ_a, is documented in detail in (ASCE 1997).

An expression for τ_a can be derived as follows. The derivation is shown only in the context of LRFD to keep the developments succinct and clear.

Generally, one can write the factored column design resistance as

$$\phi_c P_n = 0.9 \, (0.877) \, P_{e\tau} = 0.9 \, (0.877) \, \tau_a \, P_e \tag{1}$$

where 0.9 is the resistance factor in the AISC Specification for column axial compression, 0.877 is a factor applied generally to the elastic column buckling resistance in the AISC Specification to obtain the nominal column elastic buckling resistance (accounting for geometric imperfection and partial yielding effects for columns that fail by theoretical elastic buckling, as well as an implicit increased margin of safety for slender columns in AISC), and τ_a is the column inelastic stiffness reduction factor. The column inelastic buckling load, considering just τ_a and not considering the additional 0.9 and 0.877 factors, may be written as

$$P_{e\tau} = \tau_a \, P_e \tag{2}$$

where again, P_e is the theoretical column elastic buckling load.

For $\dfrac{P_{e\tau}}{P_y} > \dfrac{4}{9} \left(\dfrac{\phi P_n}{\phi P_y} > 0.390 \right)$, the AISC column inelastic strength equation may be written as

$$\frac{\phi_c P_n}{\phi_c P_y} = 0.658^{\frac{\tau_a P_y}{P_{e\tau}}} \tag{3}$$

Upon recognizing that

$$P_{e\tau} = \frac{P_n}{0.877} \tag{4}$$

this relationship may be substituted into Eq. (2), giving

$$\frac{\phi_c P_n}{\phi_c P_y} = 0.658^{\frac{0.877 \tau_a P_y}{P_n}} \tag{5}$$

Using this form of the column inelastic strength equation, one can take the natural logarithm of both of its sides, and then solve for τ_a as follows:

$$\ln\left(\frac{\phi_c P_n}{\phi_c P_y} \right) = \ln\left(0.658^{\frac{0.877 \tau_a P_y}{P_n}} \right) \tag{6}$$

$$\ln\left(\frac{\phi_c P_n}{\phi_c P_y} \right) = 0.877 \tau_a \, \frac{P_y}{P_n} \ln\left(0.658 \right) \tag{7}$$

$$\tau_a = -2.724 \, \frac{\phi_c P_n}{\phi_c P_y} \ln\left(\frac{\phi_c P_n}{\phi_c P_y} \right) \tag{8}$$

(The ϕ_c factor is included in both the numerator and denominator of the fractions in Eq. (8) to facilitate the next step of the development shown below.) The final Eq. (8) has been used widely for column inelastic buckling calculations in the context of the AISC Specification. This

equation can be applied most clearly by substituting an internal axial force γP_u for $\phi_c P_n$, such that τ_a can be thought of conceptually as an effective reduction on the member flexural rigidity (*EI*) at a given level of axial load in LRFD. As such, the τ_a equation becomes, for $\left(\dfrac{\gamma P_u}{\phi_c P_y} > 0.390 \right)$,

$$\tau_a = -2.724 \frac{\gamma P_u}{\phi_c P_y} \ln\left(\frac{\gamma P_u}{\phi_c P_y} \right) \tag{9}$$

The above equation is valid only for column buckling load levels that are within the inelastic buckling range.

For $\left(\dfrac{\gamma P_u}{\phi_c P_y} \le 0.390 \right)$, elastic buckling controls and

$$\tau_a = 1 \tag{10}$$

The above τ_a expressions can be employed with buckling analysis capabilities, such as those provided by the program Mastan (Ziemian 2014), to explicitly (or "directly") calculate the maximum column strength for any axially loaded problem.

The most streamlined application of τ_a with a buckling analysis to determine column strength is as follows:

1. Construct an overall buckling analysis model for the problem at hand. (This can be done easily for basic structural problems using programs such as Mastan.)
2. Apply the desired factored loads for a given LRFD load combination to the above model. These applied loads produce the column internal axial forces P_u.
3. Reduce the elastic modulus of the structural members, *E*, by 0.9 x 0.877 = 0.7893.
4. Reduce the moments of inertia by τ_a, based on P_u, using Eqs. (9) and (10) with $\gamma = 1$. (Alternately, steps 3 and 4 may be replaced by a single step where either the elastic modulus *E* or the moment of inertia *I* is reduced by 0.9 x 0.877 x τ_a.)
5. Solve for the inelastic buckling load of the above model. Vary the applied loads by the common scale factor γ, calculate the internal τ_a values based on the scaled load levels (using the loads γP_u), and solve for the value of γ at which the system buckles. Iterate on these calculations until the system buckles at the load level γ specified at the start of the buckling analysis. The corresponding internal axial forces γP_u in the model at incipient buckling are "directly" equal to the column axial capacities $\phi_c P_n$.

This is a very powerful approach to obtain the most accurate column design axial strengths, based on the ELM of design (AISC 2010) and including column inelastic stiffness reductions. However, the above procedure is not only valuable for determining the most accurate column ϕP_n values by the ELM. It is also very effective at assessing the design stiffness requirements for stability bracing.

Traditionally, the ELM has been used with this approach to determine the influence of end rotational restraint on columns. The restraints need not be limited to just column end rotational restraints though. When applied to column buckling problems, the above procedure gives an

accurate estimate of the maximum strength of the column accounting for the lateral restraint offered by any bracing system. The engineer simply needs to include the lateral stiffness provided by the bracing system in the buckling analysis.

In fact, if desired, rather than solving for the column buckling load for a given set of bracing stiffnesses, one can consider a given LRFD applied factored loading P_u (with $\gamma = 1$) and then solve for the required bracing stiffnesses necessary to develop the critical buckling strength equal to this factored load level. These bracing stiffnesses are commonly referred to as the *ideal bracing stiffness* values, β_i, corresponding to a given desired load level P_u.

Some engineers have suggested that $0.8\tau_b$, the general stiffness reduction used in the AISC Direct Analysis Method, should be used for all problems including calculation of column inelastic buckling loads. This is certainly possible, but such an approach misses the clear advantage of having a buckling analysis procedure that can determine directly the value of ϕP_n accounting for all end and intermediate restraint effects. This issue can be understood by comparing the net stiffness reduction factors (SRFs) $0.9 \times 0.877 \times \tau_a$ to $0.8\tau_b$ as shown in Fig. 1. The SRF $0.8\tau_b$ generally does not give an accurate estimate of the column strength ϕP_n when used in a buckling analysis calculation. Generally, it does perform reasonably well at given an appropriate estimate of the column strengths if used as part of a second-order analysis in which appropriate geometric imperfections are included per the requirements of the DM.
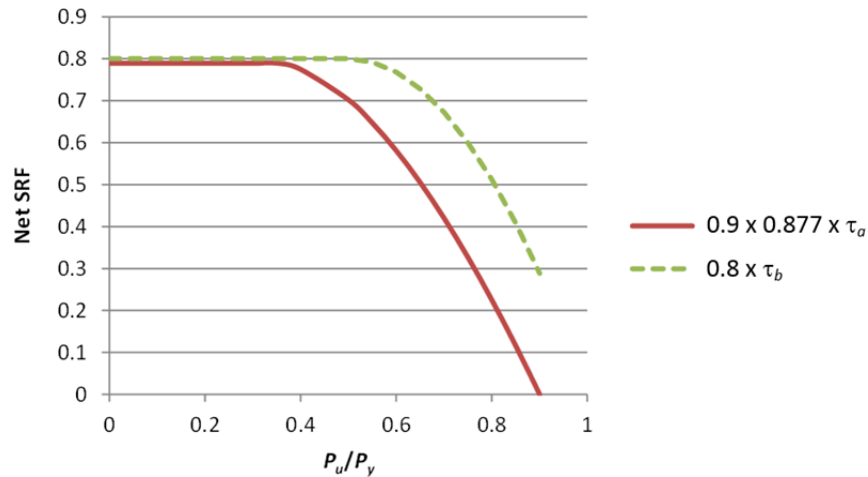

Figure 1. Comparison of the net column stiffness reduction factors (SRF) $0.9 \times 0.877 \times \tau_a$ and $0.8\tau_b$.

2.2 Inelastic Lateral Torsional Buckling Analysis using the Stiffness Reduction Obtained from the AISC LTB Strength Curves τ_{ltb}

Generally, one can write the factored AISC LRFD beam LTB design resistance as

$$\phi_b M_n = \phi_b M_{e\tau} = 0.9\tau_{ltb}M_e \tag{11}$$

where M_e represents the theoretical beam elastic LTB resistance and $M_{e\tau}$ represents the beam inelastic LTB resistance. The term τ_{ltb} is the stiffness reduction factor corresponding to the AISC LTB strength curves. The derivation of this factor parallels the derivation of the column stiffness reduction factor, τ_a, presented in Section 2.1. To keep the presentation succinct, the derivation of

τ_{ltb} is not provided here. Rather, just the resulting equations for τ_{ltb} are summarized. These equations are as follows. For all types of I-section members, when $\dfrac{\gamma M_u}{\phi_b M_{yc}} \le \dfrac{F_L}{F_{yc}}$,

$$\tau_{ltb} = 1 \tag{12}$$

However, for compact and noncompact web I-section members with $\dfrac{F_L}{F_{yc}} < \dfrac{\gamma M_u}{\phi_b M_{yc}} < \dfrac{\phi_b M_{max}}{\phi_b M_{yc}}$,

$$\tau_{ltb} = \sqrt{\dfrac{Y^4 X^2}{\left[6.76 X^2 \left(\dfrac{F_{yc}}{E} \right)^2 \left(\dfrac{\gamma M_u}{\phi_b M_{yc}} \right)^2 + 2Y^2 \right]}} \tag{13}$$

where:

$$M_{max} = R_{pc} M_{yc} \tag{14}$$

$$Y = \left[\dfrac{\left(1 - \dfrac{\gamma M_u}{\phi_b M_{yc}} \dfrac{1}{R_{pc}} \right)}{\left(1 - \dfrac{F_L}{R_{pc} F_{yc}} \right)} \left(\dfrac{L_r}{r_t} - \dfrac{L_p}{r_t} \right) + \dfrac{L_p}{r_t} \right] \left(\dfrac{\gamma M_u}{\phi_b M_{yc}} \right) \left(\dfrac{F_{yc}}{E} \right) \left(\dfrac{1}{1.95} \right) \tag{15}$$

and

$$X^2 = \dfrac{S_{xc} h_o}{J} \tag{16}$$

Conversely, for slender-web I-section members with $\dfrac{F_L}{F_{yc}} < \dfrac{\gamma M_u}{\phi_b M_{yc}} < \dfrac{\phi_b M_{max}}{\phi_b M_{yc}}$, the following simpler form is obtained in comparison to Eq. (13):

$$\tau_{ltb} = \dfrac{\gamma M_u}{\phi M_{yc}} \left[\dfrac{\left(1 - \dfrac{\gamma M_u}{\phi M_{yc}} \dfrac{1}{R_{pg}} \right)}{\left(1 - \dfrac{F_L}{F_{yc}} \right)} \left(\sqrt{\dfrac{F_{yc}}{F_L}} - \dfrac{1.1}{\pi} \right) + \dfrac{1.1}{\pi} \right]^2 \tag{17}$$

Furthermore, for compact- and noncompact-web members, one can substitute

$$\dfrac{\gamma M_u}{\phi_b M_{yc}} = \dfrac{\gamma M_u}{\phi_b M_{max} / R_{pc}} = R_{pc} \dfrac{\gamma M_u}{\phi_b M_{max}} \tag{18}$$

and for slender-web members, one can write

$$\dfrac{\gamma M_u}{\phi_b M_{yc}} = \dfrac{\gamma M_u}{\phi_b M_{max} / R_{pg}} = R_{pg} \dfrac{\gamma M_u}{\phi_b M_{max}} \tag{19}$$

These substitutions conveniently allow us to write the beam LTB inelastic stiffness reduction in terms of the independent variable $\dfrac{\gamma M_u}{\phi_b M_{max}}$, which varies over the range of 0 to 1.0.

Figures 2 and 3 illustrate how τ_{ltb} varies relative to the well-known column inelastic stiffness reduction factor τ_a for representative beam- and column-type W sections respectively. The behavior of τ_{ltb} for slender-web I-sections is similar to that shown for the beam-type W21x44 section.
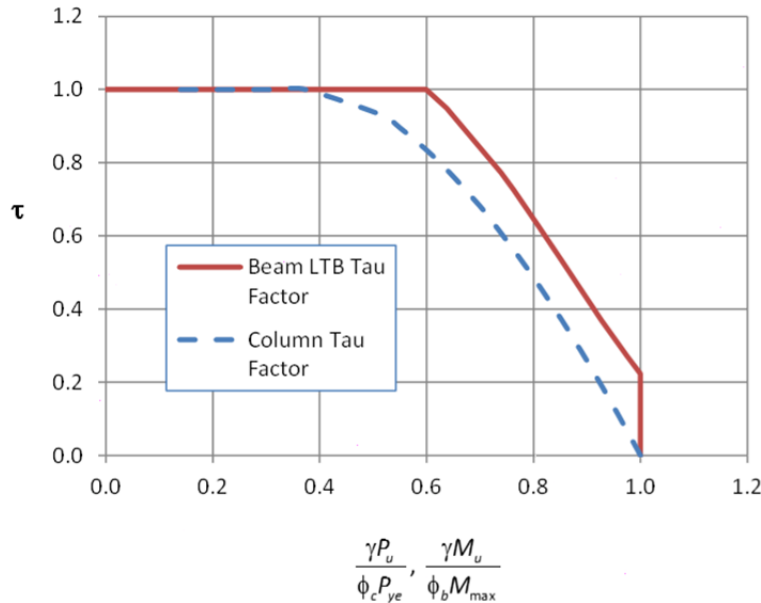

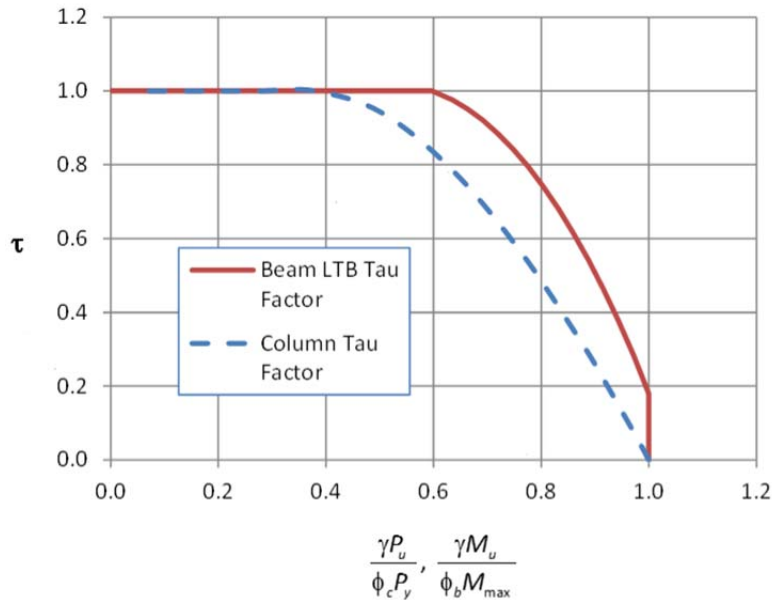Figure 2. Column and beam τ factors for a W21x44 representative beam-type wide-flange section.

Figure 3. Column and beam τ factors for a W14x257 representative column-type wide-flange section.

The LTB inelastic stiffness reduction factor, τ_{ltb}, is generally somewhat larger (i.e., reduces the capacity less) than the corresponding column inelastic stiffness reduction factor, τ_a, for a given normalized load ratio $\dfrac{\gamma P_u}{\phi_c P_{ye}}$ or $\dfrac{\gamma M_u}{\phi_b M_{max}}$. It should be noted that based on the AISC LTB strength curves, I-section beams still have significant effective inelastic stiffness when γM_u reaches the

plateau resistance $\phi_b M_{max}$. For the above W21x44 and W14x257 examples, $\tau_{ltb} = 0.223$ and 0.180 respectively when this level of loading is reached.

When used with a buckling analysis, if the maximum moment at incipient buckling, γM_u, is larger than $\phi_b M_{max}$ in an analysis in which all the τ_{ltb} values are based on the corresponding internal moments, the member has reached the "plateau LTB strength"; hence, the design strength is equal to $\phi_b M_{max}$.

For proper calculation of the LTB resistance from a buckling analysis, several requirements must be satisfied:

1. The buckling analysis software has to rigorously include the contributions from warping rigidity EC_w as well as the St. Venant torsional rigidity GJ and the lateral bending rigidity EI_y in the context of doubly-symmetric I-section members.
2. In addition, for singly-symmetric I-section members, the buckling analysis must account rigorously for the behavior associated with the shear center differing from the cross-section centroidal axis, which relates to the monosymmetry factor, β_x, in rigorous analytical equations for the LTB resistance of these types of beams.
3. The τ_{ltb} factor is applied equally to all the member elastic stiffness contributions (GJ, EC_w and EI_y) for the execution of the buckling analysis. Physically, it can be argued that the effective reduction in the St. Venant torsional rigidity of an inelastic beam is not as large as the reduction in the effective EI_y and EC_w values. However, the use of an equal reduction on all three rigidities (at a given cross-section) is simple and sufficient. Furthermore, equal reduction on all three cross-section rigidities produces the beam LTB resistance from the AISC Specification equations exactly for cases involving uniform bending and simply-supported end conditions.
4. The internal force state upon which the buckling analysis is based is to be determined using the elastic properties of the structure, as in current practice. This requirement can be waived for statically determinate structures or structural systems. However, when conducting a buckling analysis of an indeterminate structure, it is essential that the elastic member properties are used for determining the internal forces. Otherwise, the member internal force relationships will be influenced by the distribution of the internal inelastic stiffnesses, which is not considered necessary or appropriate for elastic design. (This statement also applies to general column inelastic buckling)

The above requirements can be satisfied with the Mastan software (Ziemian 2014) for doubly-symmetric beams; hence, Mastan is used for the example presented in this paper. The software SABRE2 (Jeong 2014), provides rigorous buckling analysis capabilities for general singly-symmetric and non-prismatic beam cases.

A sufficient number of elements per member must be employed for the above LTB solutions. For frame elements based on thin-walled open-section beam theory and cubic Hermitian interpolation of the transverse displacements and twists along the element length (the type of frame element employed by Mastan), four elements within each unbraced length tend to be sufficient. In addition, for inelastic buckling cases involving a moment gradient, the variation of the inelastic stiffness along the member length must be captured. Twenty elements with each

span between the major-axis bending support locations tend to be sufficient for problems that do not have any reversal of the sign of the moment within the span. Thirty elements within each span between the major-axis bending support locations tend to be sufficient for problems involving fully-reversed curvature bending. The τ_{ltb} factors are to be calculated based on the internal forces at the mid-length of each the frame elements. If frame elements are used that employ numerical integration along the element length (as in SABRE2), the internal forces at each of the integration points may be used (this provides additional solution accuracy).

Obviously, the above inelastic LTB solutions are not manual engineering solutions. However, for that matter, neither is the general second-order elastic analysis of an indeterminate frame. Although engineers can conduct approximate analysis to perform initial sizing of the members in an indeterminate frame structure, they do not generally rely on these analyses, manual moment distribution calculations, etc. for final design at this day and time. With the appropriate software implementation of the above τ_{ltb} calculations using a frame element based on thin-walled open-section beam theory, the above procedure is quite easy to apply. The software performs the appropriate elastic matrix analysis of the structure to determine the required member internal forces. Then the software performs an inelastic eigenvalue buckling analysis based on these forces to evaluate the design. If the software automatically handles the internal inelastic stiffness reductions based on the magnitude of the internal forces, the inelastic buckling analysis is relatively straightforward to apply.

This approach can be quite powerful to provide highly accurate assessments of end restraint, continuity, general moment gradient and finite bracing stiffness effects on the LTB resistance of beam and frame members. One key attribute of the power of this approach is that, similar to the τ_a approach for column buckling, once one has determined the load level corresponding to incipient inelastic buckling using the τ_{ltb} factor, the internal forces in the model at the buckling load correspond precisely to the design moment resistances $\phi_b M_n$. Furthermore, this approach allows the consideration of any and all restraints from bracing and member end conditions to be directly and automatically considered in the design assessment, by including them in the structural analysis model. Regarding the assessment of the required stiffness for stability bracing, this assessment is accomplished as a direct and integral part of the calculation of the member LTB resistances. If the load parameter γ is greater than 1.0 from the buckling analysis, with the internal element stiffnesses calculated based on the τ_{ltb} equations given the internal forces at the load level γ, then the beam member has sufficient design strength for LTB. (Note that other limit states including flange local buckling, web crippling, connection limit states, etc. must be checked separately, just as they would be in ordinary design.)

If desired, rather than solving for the beam LTB load given bracing stiffnesses, one can consider a given LRFD applied factored loading M_u (with $\gamma = 1$) and then solve for ideal bracing stiffnesses necessary to develop this factored load level at buckling. The ideal bracing stiffnesses are then multiplied by $2/\phi$ to obtain the required bracing stiffness for design.

2.3 Validation and Demonstration of LTB Stiffness Reduction Equations

Consider the LTB resistance of W21x44 beams having torsionally and flexurally simply-supported end conditions and unbraced lengths ranging from zero to 20 ft. Figure 4 shows the

results for the uniform bending case as well as a basic moment gradient case involving an applied moment at one end and zero moment at the other end of the beams.
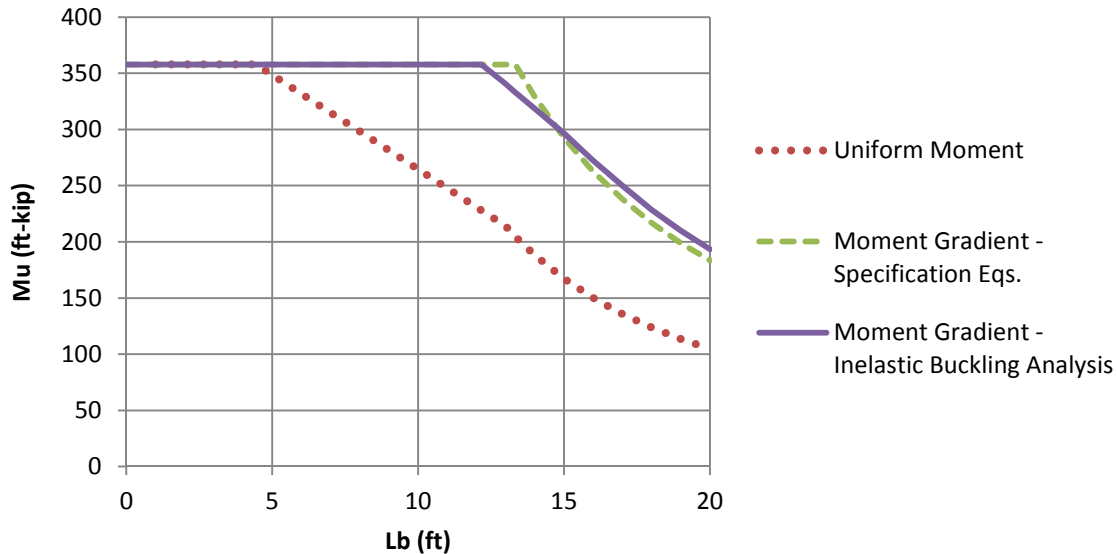

Figure 4. Lateral Torsional Buckling design resistances for W21x44 beams (F_y = 50 ksi), calculated using the AISC Specification equations and using a buckling analysis with the corresponding stiffness reduction factor $0.9\tau_{ltb}$.

The following observations can be made from this LTB study:

1. The buckling analysis results for the LTB resistance under uniform bending match exactly with the calculations from the AISC Specification Section F2 equations. Therefore, only one curve is shown for the uniform bending case in Fig. 4.
2. The buckling analysis results for the LTB resistance under the moment gradient fit closely with the calculations from AISC Specification Section F2 using a moment gradient factor C_b = 1.75. However, this LTB curve is slightly different from the one obtained using the Section F2 LTB equations directly. The differences between these curves are important, and may be explained as follows:
   a. For longer unbraced lengths, where the beam is elastic and τ_{ltb} = 1, the buckling load determined from Mastan is approximately 6 % larger than the capacity determined from the AISC Section F2 equations with C_b taken as 1.75. The Mastan solution is a more accurate assessment in this case. The 1.75 value for C_b is a lower-bound approximation developed by Salvadori (1955). The Mastan solution is approximately 11 % larger than the solution with C_b = 1.67 obtained from AISC Eq. (F1-1) for this problem. AISC Eq. (F1-1), originally developed by Kirby and Nethercot (1979), gives a "lower" lower-bound solution than Professor Salvadori's equation for this problem.
   b. For intermediate unbraced lengths at which the maximum moment at incipient buckling is larger than $\phi_b F_L S_{xc} = 0.9(0.7 F_y S_{xc})$ (equal to 214 ft-kip for the W21x44), the inelastic buckling analysis solution is again fully consistent with the AISC Section F2 equations, but is a more accurate assessment of the LTB resistance than the direct use of the AISC Section F2 equations. In this case, as the buckling resistance increases above $\phi_b F_L S_{xc}$, some reduction in the LTB resistance occurs due to the onset of yielding at the locations where the internal moment is largest. The approach taken in AISC Chapter F is to simply scale the uniform bending LTB resistance by C_b, but with a cap of $\phi_b M_{max}$ on the

10

maximum flexural resistance. As discussed by Yura et al. (1978), this approach tends to over predict the true response to some extent in the vicinity of where the elastic or inelastic LTB design strength curve intersects $\phi_b M_{max}$, although the approximation is considered to be acceptable. The LTB resistances obtained from the buckling analysis are slightly smaller than those obtained directly from the AISC Chapter F2 equations in the vicinity of the location where the LTB resistance reaches its plateau resistance $\phi_b M_{max}$, reflecting the more rigorous accounting for inelastic stiffness reduction effects on the LTB resistance in the buckling analysis based solution.

3. Beam Torsional Bracing Example

3.1 Problem Description
The grillage shown in Fig. 5, which is similar to a beam torsional bracing example presented in AISC (2002), supports glass roof panels subjected to uniformly distributed load. The W30x90 members (F_y = 50 ksi) are flexurally and torsionally simply-supported at their ends and are subjected to a maximum internal moment of M_u = 850 ft-kip (> $\phi_b M_n$ = 144 ft-kip for L_b = 60 ft and C_b = 1.14). Therefore, bracing is needed from the secondary W12x40 beams (F_y = 50 ksi).
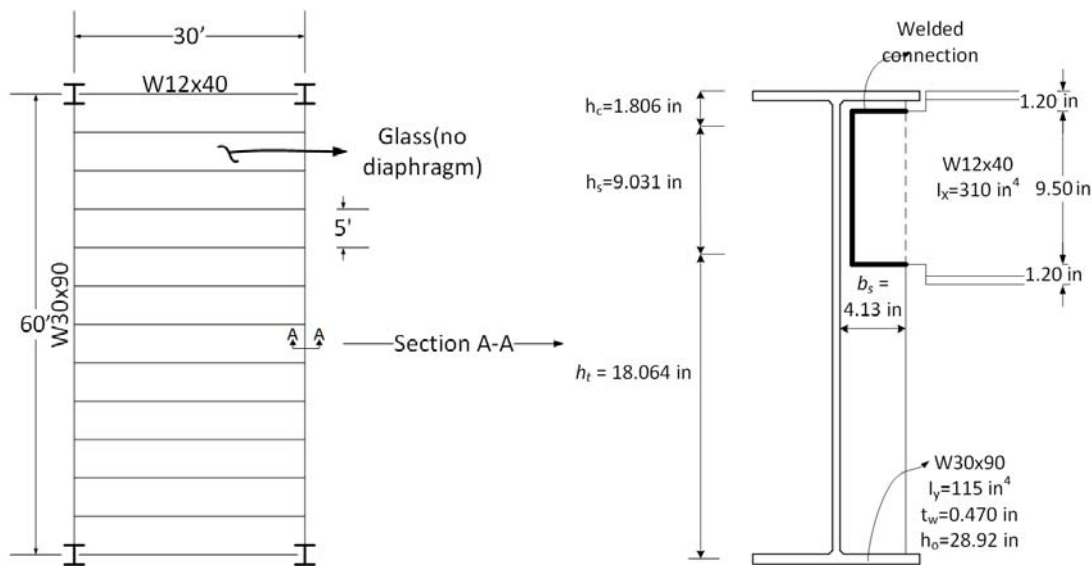

Figure 5. Beam Torsional Bracing Example.

The W12x40 beams have ample stiffness to brace the W30x90 members, but only if the connections are sufficient and the distortional flexibility of the W30x90 cross-section does not overly limit the effective torsional bracing stiffness.

The relevant properties and dimensions for this problem are as follows:
  E = 29,000 ksi
  L = 60 ft.   overall length of the W30x90 beams
  h_o = 28.9 in.   distance between the mid-thickness of the W30x90 flanges
  t_w = 0.470 in.   web thickness of the W30x90 beams
  I_y = 115 in^4 lateral bending moment of inertia of the W30x90 beams

$I_b = 310$ in^4 moment of inertia of W12x40 secondary beams

$L_b = 30$ ft.   length of the secondary beams

Full-depth one-sided transverse stiffeners (4.13 in x 0.375 in) are used at each of the secondary beam locations as shown in Fig. 5. The height h_s is idealized as a length over which the web of the W30x90 is rigidly constrained to deflect in a straight line (due to the additional stiffening coming from the welded connection to the W12x40 beam webs). The torsional bracing is modeled as a rotational spring at the middle of this length.

3.2 Assessment using AISC Appendix 6 with refinements from Yura (2001) and AISC (2002)
Given the idealization summarized in Section 3.1, the effective torsional bracing stiffness provided by the secondary beams and their connection to the W30x90 girders may be calculated as follows (Yura 2001):

$$\beta_c = \frac{3.3E}{h_c}\left(\frac{h_o}{h_c}\right)^2\left(\frac{1.5h_c t_w^3}{12} + \frac{t_s b_s^3}{12}\right) = 30{,}180{,}000\ \frac{\text{in-kip}}{\text{rad}} \tag{20}$$

$$\beta_t = \frac{3.3E}{h_t}\left(\frac{h_o}{h_t}\right)^2\left(\frac{1.5h_t t_w^3}{12} + \frac{t_s b_s^3}{12}\right) = 33{,}030\ \frac{\text{in-kip}}{\text{rad}} \tag{21}$$

$$\beta_b = \frac{6EI_b}{L_b} = 149{,}800\ \frac{\text{in-kip}}{\text{rad}} \tag{22}$$

$$\beta_{Tprov} = \frac{1}{\dfrac{1}{\beta_c} + \dfrac{1}{\beta_t} + \dfrac{1}{\beta_b}} = 27{,}040\ \frac{\text{in-kip}}{\text{rad}} \tag{23}$$

Any distortional flexibility of the beam within the height of the connection region h_s, as well as the torsional flexibility of the overall girder system due to differential major-axis bending of the girders, is assumed to be negligible.

As explained in AISC (2002), the required torsional bracing stiffness can be determined most accurately from the following refinement of the AISC Specification Appendix 6 Eq. (A-6-11):

$$\beta_T = \frac{1}{\phi}\left[\frac{2.4L\left(M_u - \phi_b M_{no}\right)^2}{nEI_{yeff}C_b^2}\right] = 4508\ \frac{\text{in-kip}}{\text{rad}} \tag{24}$$

where:

$\phi = 0.75$

$L = 60$ ft.   overall W30x90 span length

$M_u = 850$ ft-kip   for the specified factored design loading

$\phi_b M_{no} = 144$ ft-kip   strength of the W30x90 in the absence of any intermediate

                               bracing, including the associated moment gradient factor $C_{bu} = 1.14$

$n = 11$ number of intermediate brace points

$I_{yeff} = I_y = 115$ in^4 lateral bending moment of inertia of the W30x90 beams

and

$C_b = 1.0$ moment gradient factor, based on near uniform bending at the

                               mid-span unbraced lengths of the W30x90 beams

Therefore, it can be concluded that the W30x90 beam and the above bracing system has adequate stiffness to resist the required loads corresponding to $M_u = 850$ ft-kip. If an unstiffened connection detail such as the one evaluated in AISC (2002) is considered for this problem, the distortional flexibility of the W30x90 web severely limits the effective torsional bracing stiffness such that the unstiffened detail will not for the above level of loading.

From recommended AISC 2016 provisions (AISC 2015), the bracing strength requirement for this case is

$$M_{br} = 0.02M_u = 17.0 \text{ ft-kip} \tag{25}$$

The subsequent test simulation solutions indicate a strength requirement in this problem of 2.2 % of the maximum moment to develop the limit load capacity of the W30x90 beams. This is based on an out-of-alignment of the top flange of 30 ft x 12in/ft x 1/500 = 0.72 inches at the girder mid-span, which corresponds to a twist imperfection of $\theta_o = 0.72$ in. / 28.9 in. = 0.0249 rad given that the bottom flange is assumed to have zero out-of-alignment. This twist imperfection is slightly smaller than the net rotation assumed in AISC (2002) considering movement in the bolted connections of the W12x40 beams due to hole clearances. However, 99 % of the flexural capacity is developed when the bracing moment reaches 2.0 %. Therefore, 2.0 % is considered an acceptable required strength for the stability bracing design in this problem.

Given the above strength requirement, a welded connection can be designed to transfer the required shears and moments to the W12x40 beams. The 4.33 x 0.375 inch transverse stiffeners on the W30x90 beam are sufficient to transfer the bracing moment M_{br} to the main girders, but they actually start to yield at slightly larger than 2.0 % bracing moment, as discussed subsequently. Also, the 9.5 inch depth of the coped W12x40 web is adequate to transfer the required moment.

3.3 Assessment via Buckling Analysis
To perform a design assessment for this problem using a buckling analysis, one can execute the following steps:

1. Construct a buckling analysis model of one of the W30x90 beams, including the modeling of the effective elastic rotational restraint at the attachments to the W12x40 secondary beams. Since $M_u = 850$ ft-kip is greater than $0.7\phi_b M_y = 643$ ft-kip for the W30x90, the primary beams have significant inelastic stiffness reduction at their mid-span at the required load level. Figure 6 shows the $0.9\tau_{ltb}$ values determined at the mid-length of each of the 24 elements used for the buckling analysis of the W30x90 beam. These $0.9\tau_{ltb}$ values are to be applied to *all* the beam cross-section rigidities associated with LTB (*GJ*, EC_w and EI_y). For this problem, the simplest way to accomplish this is to apply these reductions to the elastic modulus E for each of the 24 beam elements.
2. Apply the factored loading of $q_u = 1.890$ klf to the model, which produces $M_u = 850$ ft-kip at the member's mid-span. This load can be applied with sufficient accuracy by applying concentrated loads of 9.444 kip at each of the W12x40 beam connection locations.
3. Reduce the W30x90 elastic rigidity contributions *GJ*, EC_w and EI_y by $\phi_b\tau_{ltb} = 0.9\tau_{ltb}$ in each of the frame elements used to model the member. Although this step requires some effort to

set these values manually, this calculation can be included easily as part of a fast streamlined inelastic buckling analysis software procedure.

4. Vary the effective elastic rotational stiffness at the secondary beam connection locations until the model buckles at the above required load. The corresponding bracing stiffness is the ideal bracing stiffness β_{Ti} required to develop the above applied loading. The ideal bracing stiffness obtained from this assessment is

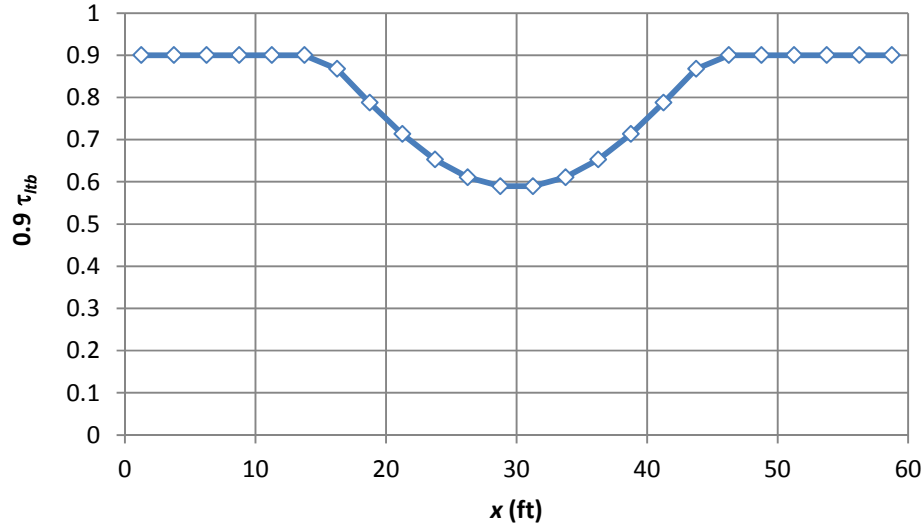$$\beta_{Ti} = 2463 \frac{\text{in-kip}}{\text{rad}} \tag{26}$$

Figure 6. Variation of $0.9\tau_{ltb}$ along the length of the W30x90 primary beams due to the variation in $M_u/\phi M_n$ along the member length.

5. Apply the conventional factor $2/\phi$ to the ideal bracing stiffness obtained from the above buckling analysis to obtain the required bracing stiffness.

$$\beta_T = \frac{2}{\phi}\beta_{Ti} = 6568 \frac{\text{in-kip}}{\text{rad}} \tag{27}$$

This value can be compared to the value of 4508 in-kip/rad obtained from Eq. (24) in Section 3.2. The above value is considered to be a more accurate estimate of the required torsional brace stiffness, since it is obtained from a rigorous buckling analysis model, particularly since the rigorous buckling analysis accounts for LTB inelastic stiffness reduction as illustrated in Fig. 6 whereas Eq. (24) does not include any accounting for the effect of beam inelasticity. Equation (24) assumes that the W30x90 beam's elastic stiffness is available to resist the brace point lateral displacements throughout the member length. Prado and White (2014) and Lokhande and White (2014) show from extensive parametric test simulations that the torsional bracing requirements are indeed influenced by beam inelasticity.

6. Compare the above required torsional bracing stiffness to the provided torsional bracing stiffness, including the consideration of distortional flexibility of the stiffened W30x90 cross-section at the brace points. The calculation of the provided torsional bracing stiffness is given by Eq. (23).

Since β_{Tprov} is significantly greater than the above β_{br}, we can conclude that the W12x40 secondary beams combined with the one-sided 4.13 x 0.375 inch full-depth transverse stiffeners provide ample stiffness to develop the required design load associated with $M_u = 850$ ft-kip in the W30x90 beams.

Based on recommended AISC 2016 Appendix 6 provisions (AISC 2015), the bracing strength requirement is the same as in Section 3.3.1 Eq. (25), i.e., $M_{br} = 0.02M_u = 17.0$ ft-kip.

It should be noted that the above model provides a direct assessment of the W30x90 beam LTB resistances. No separate check of the Specification LTB strength equations is necessary once these calculations have been performed. This assessment includes a rigorous assessment of the influence of the torsional bracing stiffnesses as well as continuity effects between the adjacent unbraced lengths along the span. As noted previously, strength limit states other than LTB must still be checked.

Another powerful feature of the inelastic buckling solution is that it can be used to justify the stiffening of the W30x90 web at only a selected number of secondary beam locations (rather than providing the same stiffening at each of W12x40 beams). This solution is not shown here in the interest of keeping the presentation brief. Equation (24) is based on the assumption of equally-spaced equal-stiffness torsional bracing throughout the span of the beam that is being braced. In addition, Eq. (24) is an entirely elastic derivation, involving the implicit assumption that the elastic stiffness of the primary beam is available to help resist the brace point displacements, as well as the assumption that the beam strength is scaled by C_b, regardless of whether the "plateau LTB resistance" ($\phi_b M_p$ for a compact-section beam) is exceeded.

3.3 Comparisons to Test Simulations
Figure 7 plots the moment at the mid-span of the W30x90 beams versus the maximum bracing moment in the secondary beams, expressed as a percentage of the W30x90 mid-span moment. The curves in this plot are obtained from four separate test simulations. The test simulations are refined spread-of-plasticity structural analyses, conducted using the S4R general purpose shell element in ABAQUS (Simulia 2013), including specified initial geometric imperfections and residual stresses as discussed below and following the requirements of Appendix 1 of the AISC Specification. The results are generated considering the two different geometric imperfections shown in Fig. 8. The "larger" of these imperfections involves an equal out-of-alignment of 1/500 in all of the unbraced lengths on each side of the mid-span, resulting in an overall Δ_o of the top flange of 0.72 inch at the mid-span, as discussed previously. The "smaller" of these imperfections involves an out-of-alignment of 1/500 only in the $L_{br} = 5$ ft unbraced lengths on each side of the critical brace at the W30x90 mid-span. In addition, a top-flange out-of-straightness of $L_{br}/2000 = 0.03$ inch is specified in opposite directions in the unbraced lengths on each side of the mid-span (this imperfection is used, rather than $L_{br}/1000$, as a representative average out-of-straightness within the unbraced lengths). The bottom flange is modeled as perfectly straight in all of these simulations. Both of these imperfection patterns satisfy the AISC Code of Standard Practice (COSP) tolerances. In addition, results are generated with the one-sided stiffener having the actual yield strength of $F_y = 50$ ksi and with the stiffener modeled as infinitely elastic.

For the residual stresses used in the test simulations, 0.9 times 0.5 of the Lehigh residual stress pattern is employed. The 0.9 factor corresponds to factoring of the material strength ordinates by 0.9 as required by Appendix 1 of the AISC Specification. One-half of the magnitude of the residual stresses in the Lehigh residual stress pattern is used because this value of the residual stresses tends to produce test simulation results that match reasonably well with the AISC LTB strength curves, which in turn capture very close to the mean LTB resistances obtained from experimental tests (White and Jeong 2008; White and Kim 2008; Subramanian and White 2015).
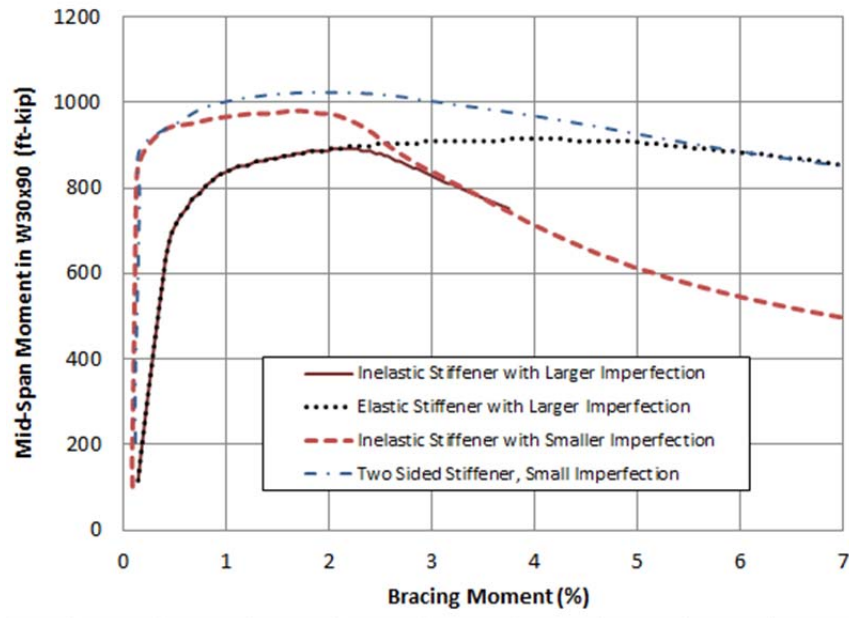

Figure 7. Mid-span internal moment in the W30x90 primary beams versus the largest bracing moment in the secondary W12x40 beams (occurring in the bracing beam attached at the mid-span) from four different test simulations.
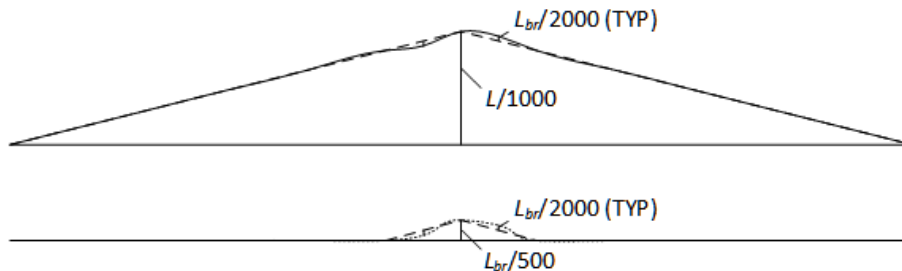

Figure 8. "Larger" and "smaller" out-of-plane initial geometric imperfection displacements considered on the top flange of the W30x90 beams ($L_{br} = 5$ ft and $L = 60$ ft).

Figure 7 shows that the W30x90 is sufficient to develop the required moment capacities for the design scenario considered. However, the maximum capacity of the W30x90 beams is less than $\phi_b M_p = 1061$ ft-kip, although if one checks the AISC Appendix 6 bracing requirements to develop $\phi_b M_p$, it can be concluded that the bracing stiffness provided should be sufficient to develop the factored plastic moment capacity. The larger imperfection case with inelasticity modeled in the stiffener shows the smallest strength of $M_{max} = 897$ ft-kip. If the stiffener is assumed to be infinitely elastic, only a slightly larger strength of $M_{max} = 915$ ft-kip is developed.

It is determined that the selected imperfection has a significant impact on the maximum capacity of the primary beams. If the smaller imperfection is considered, the system develops an M_{max} = 980 ft-kip in the W30x90 beams, still 8 % smaller than $\phi_b M_p$. Therefore, an additional test simulation is conducted with the smaller imperfection and in which a double-sided transverse stiffener is used that has a total width equal to the 10.4 inch width of the W30x90 flanges at each of the bracing locations. This case develops an M_{max} of 1024 ft-kips, which is within 3.5 % of the factored design plastic moment.

For the beams with the one-sided stiffener, larger imperfections, and either actual or infinitely elastic properties, the required bracing moment in the secondary beams is 1.4 % of M_u (11.9 ft-kip) at M_u = 850 ft-kip. If the maximum capacity of the "elastically-stiffened" beam of 915 ft-kip were utilized, a required bracing moment of 4.2 % (38.43 ft-kip) would be required. Nevertheless, 97 % of this member's moment capacity is developed (i.e., 886 ft-kip) when the bracing required moment reaches 2.0 % of the girder mid-span moment, and this result is obtained for both the solutions with the elastic as well as the inelastic stiffener. Generally, a required bracing moment of 2.0 % has been found to be acceptable as a simple estimate for all cases, based on the criterion that at least 95 % of the maximum moment capacity is developed in the member that is being braced (Prado and White 2014; Lokhande and White 2014).

Figure 7 shows that at slightly more than 2 % bracing moment, the actual 4.13 x 0.375 inch one-sided stiffener starts to yield in the case where the beam has the larger imperfection, thus limiting the maximum capacity of the W30x90 beams to 897 ft-kip and resulting in a bracing moment at the primary beam limit load of only 2.2 %.

In addition, Fig. 7 shows that the bracing moments are significantly smaller for the beams with the smaller imperfection until just before the maximum capacity of the beams is achieved. The torsional bracing moments at the limit load for the beams with the smaller imperfection are 1.8 % when the one-sided stiffener is used, and 1.9 % when the large two-sided stiffener is used. However, at 95 % of the maximum capacity of these beams, the torsional bracing moments are only 0.7 % and 0.4 % respectively.

3.4 Additional Comparisons to Test Simulation Results
Figure 9 shows the maximum strength of the W30x90 beams versus the total effective torsional bracing stiffness, obtained from: (1) the AISC Appendix 6 provisions, (2) the above Buckling Analysis procedures, and (3) refined Test Simulation calculations. These curves consider a scenario in which the size of the secondary bracing beams is varied, giving an overall variation in β_{Tprov}. These types of curves are often referred to as "knuckle curves" in the literature. For the Appendix 6 calculations, given a total effective bracing stiffness β_{Tprov}, Eq. (24) is solved for M_u to generate the points along the Appendix 6 knuckle curve. For the Buckling Analysis calculations, the procedure outlined earlier is employed, but with a variable β_b. For the Test Simulation solutions, the 4.13 x 0.375 inch one-sided stiffener results are considered with the larger and smaller imperfections shown in Fig. 8. In addition, the 10.4 x 0.375 inch two-sided stiffener results are shown for the smaller imperfection.

Figure 9 is helpful to understand the behavior associated with the Appendix 6 and Buckling Analysis solutions, and the inability of the W30x90 beams to develop $\phi_b M_p$ in spite of the use of large torsional bracing stiffness values. The following points can be gleaned from this plot:

- The refined AISC Appendix 6 Eq. (23) suggests that the W30x90 beams are able to develop $\phi_b M_p$ = 1061 ft-kip at a relatively small effective torsional bracing stiffness value of only 7605 in-kip/rad. This behavior is related to the fact that Eq. (23) assumes fully elastic behavior of the W30x90 beams, whereas the beams have substantial inelastic stiffness reduction as they approach $\phi_b M_p$ = 1061 ft-kip at their mid-span.
- The Buckling Analysis solution, based on the use of reduced stiffnesses of $0.9\tau_{ltb}$ as a function of the internal moment levels along the W30x90 beams, predicts that the primary beams are able to develop $\phi_b M_p$ = 1061 ft-kip at an ideal brace stiffness of β_{Ti} = 11,980 in-kip/rad., which then translates to a required bracing stiffness of

$$\beta_T = \frac{2\beta_{Ti}}{\phi} = 31{,}920\,\frac{\text{in-kip}}{\text{rad}} \tag{28}$$

- The knuckle curve determined by the Buckling Analysis procedure does a reasonable job of capturing the shape of the test simulation based knuckle curves for the larger imperfection. However, the Buckling Analysis solution predicts that the W30x90 beams can achieve $\phi_b M_p$ for effective torsional brace stiffnesses β_T greater than 31,920 in-kip/rad, whereas the test simulations with the larger imperfection only achieve a maximum resistance of 897 and 915 ft-kip at an effective torsional bracing stiffness of approximately 22,000 in-kip/rad. With the smaller imperfection and the large two-sided transverse stiffener, the W30x90 beams reach a maximum strength of 1024 ft-kip at a β_T of approximately 22,000 in-kip/rad.
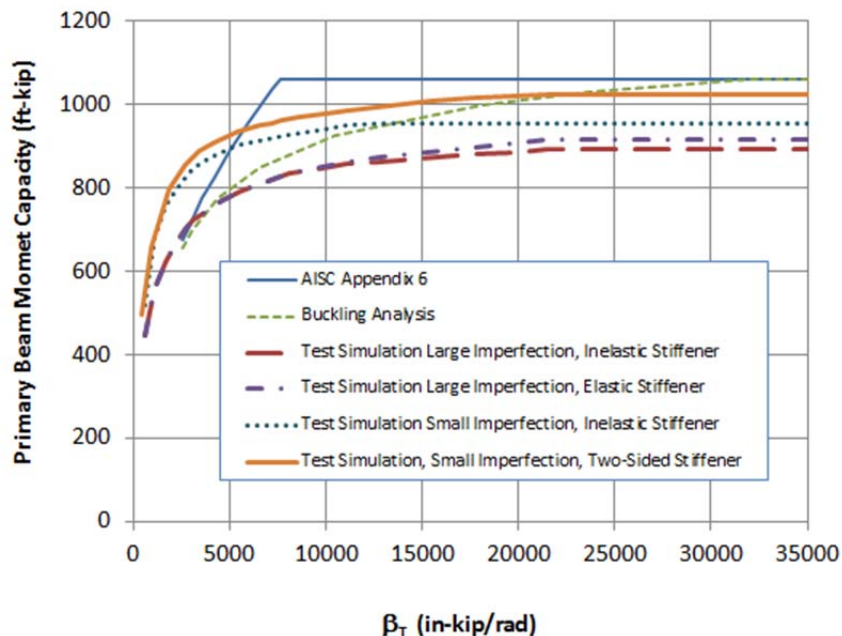

Figure 9. W30x90 beam design strength versus total effective torsional bracing stiffness knuckle curves from Appendix 6 and Buckling Analysis and Test Simulations,.

18

Several potential underlying reasons for the mid-span moment at the limit load being significantly smaller than $\phi_b M_p$ in the test simulations are as follows:

a) Test simulations based on geometric imperfections set at the AISC Code of Standard Practice maximum tolerances and using common traditional nominal residual stress patterns commonly indicate some difficulty in reaching $\phi_b M_p$ at unbraced lengths close to L_p for problems with uniform or near uniform bending. For the W30x90 beams used here, $L_p = 7.38$ ft however, whereas the unbraced length employed in this example is $L_{br} = 5$ ft. Therefore, the considerations appear to be deeper than just the conservative nature of typical test simulation results involving near uniform bending.

b) Rigid bracing benchmark results shown in Prado and White (2014) indicate that there is some minor variation in the maximum strength achieved for beams with both flanges restrained laterally, only the compression flange restrained laterally, or only twisting of the member restrained at the brace points. The rigid bracing strengths for torsional bracing are the smallest, and the rigid bracing strengths with both flanges restrained laterally are the largest. This type of behavior would appear to be a factor in the maximum strengths reached in this problem as well, but based on Prado and White (2014), it would not be expected that this behavior is the major reason why the W30x90 beams do not reach $\phi_b M_p$ in this example.

c) The "larger" imperfections result in a value of θ_o at the mid-span of the W30x90 girders that is relatively large compared to their 5 ft unbraced lengths. By considering the smaller imperfections, the strengths are increased measurably; however, the most substantial increase is obtained when the girders are also heavily stiffened at the torsional bracing locations. It is apparent that the test simulation beam strengths in this example problem are sensitive to both the overall geometric imperfection as well as the stiffening of the beam cross-section. As such, it is recommended that maximum limits on θ_o, or θ_o/L_{br} should be considered by the COSP. In addition, it is suggested that the sensitivity of beam strengths to cross-section distortion when torsionally-braced I-section beams are loaded to moment levels involving substantial cross-section plasticity

The above sensitivities to θ_o and the beam cross-section stiffening highlight the limitations of common member resistance equations in design codes in general. Common resistance equations do not capture any variation in the member capacity as a function of these types of parameters. Refined test simulation solutions, which are permitted by AISC Appendix 1, can account for these effects. However, these types of solutions are certainly not routine.

4. Conclusion

This research addresses the proper configuration of a buckling analysis to determine the maximum buckling strength of columns and beams directly, accounting rigorously for all restraints coming from bracing and unbraced length end conditions, without the need to separately evaluate the resistances using the AISC design strength equations. In addition the proposed method can be used to assess the required stiffness of stability bracing within the same analysis. An example design problem is presented that suggests some additional consideration should be given to twist imperfection magnitudes and potential imperfection sensitivities in torsionally braced beams.

In ongoing research, the authors are pursuing the development of prototype computer-aided engineering software that facilitates the rapid application of these procedures, including the extension of these methods to the design of beam-columns.

References

AISC (2015), "Specification for Structural Steel Buildings," Ballot 3 Manuscript of the 2016 Specification, American Institute of Steel Construction,

AISC (2010). "ANSI/AISC 360-10 Specification for Structural Steel Buildings", American Institute of Steel Construction, Chicago, IL

AISC (2002). "Example Problems Illustrating the Use of the New Bracing Provisions – Section C3, Spec and Commentary", Ad hoc Committee on Stability Bracing, November.

ASCE (1997). *Effective Length and Notional Load Approaches for Assessing Frame Stability: Implications for American Steel Design*, Task Committee on Effective Length, Technical Committee on Load and Resistance Factor Design, Structural Engineering Institute, American Society of Civil Engineers, Reston, VA.

Bishop, C.D. (2013). "Flange Bracing Requirements for Metal Building Systems", Doctoral Dissertation, Georgia Institute of Technology, Atlanta, GA.

Kirby, P.A. and Nethercot, D.A. (1979). *Design for Structural Stability*, Wiley, New York.

Lokhande, A.M. and White, D.W. (2014). "Evaluation of Steel I-Section Beam and Beam-Column Bracing Requirements by Test Simulation,",Research Report to the American Institute of Steel Construction. School of Civil and Environmental Engineering, Georgia Institute of Technology, Atlanta, GA.

Prado, E.P. and White D.W. (2014). "Assessment of Basic Steel I-Section Beam Bracing Requirements by Test Simulation" Research Report to the American Institute of Steel Construction, School of Civil and Environmental Engineering, Georgia Institute of Technology, Atlanta, GA.

Jeong, W.Y. (2014). "Structural Analysis and Optimized Design of General Nonprismatic I-Section Members," Doctoral Dissertation, School of Civil and Environmental Engineering, Georgia Institute of Technology, Atlanta, GA.

Salvadori, M.G. (1955). "Lateral Buckling of Beams," Transactions ASCE, Vol. 120, 1165.

Simulia (2013). ABAQUS/Standard Version 6.12-1, Simulia, Inc., Providence, RI.

Yura, J.A., Galambos, T.V. and Ravindra, M.K. (1978). "The Bending Resistance of Steel Beams," Journal of the Structural Division, ASCE, 104(ST9), 1355-1370.

Yura, J.A. (2001). "Fundamentals of Beam Bracing," Engineering Journal, AISC, 38(1), 11-26.

Ziemian, R.D. (2014). "MASTAN2 v3.3," <www.mastan2.com> (Jan 17, 2015).